J. Am. Soc. Mass Spectrom. (2016) 27:220–232
DOI: 10.1007/s13361-015-1286-8

RESEARCH ARTICLE

Comprehensive Characterization of AMP-Activated Protein Kinase Catalytic Domain by Top-Down Mass Spectrometry

Deyang Yu,[1,2] Ying Peng,[1,5] Serife Ayaz-Guner,[1,5] Zachery R. Gregorich,[1,3] Ying Ge[1,2,3,4,5]

[1]Department of Cell and Regenerative Biology, School of Medicine and Public Health, University of Wisconsin-Madison, Madison, WI 53706, USA
[2]Molecular and Environmental Toxicology Training Program, University of Wisconsin-Madison, Madison, WI 53706, USA
[3]Molecular and Cellular Pharmacology Training Program, University of Wisconsin-Madison, Madison, WI 53706, USA
[4]Department of Chemistry, University of Wisconsin-Madison, Madison, WI 53706, USA
[5]Human Proteomics Program, School of Medicine and Public Health, University of Wisconsin-Madison, Madison, WI 53706, USA

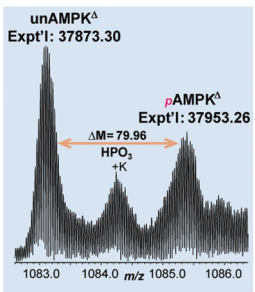

Abstract. AMP-activated protein kinase (AMPK) is a serine/threonine protein kinase that is essential in regulating energy metabolism in all eukaryotic cells. It is a heterotrimeric protein complex composed of a catalytic subunit (α) and two regulatory subunits (β and γ). C-terminal truncation of AMPKα at residue 312 yielded a protein that is active upon phosphorylation of Thr172 in the absence of β and γ subunits, which is refered to as the AMPK catalytic domain and commonly used to substitute for the AMPK heterotrimeric complex in in vitro kinase assays. However, a comprehensive characterization of the AMPK catalytic domain is lacking. Herein, we expressed a His-tagged human AMPK catalytic domin (denoted as AMPK$^{\Delta}$) in *E. coli*, comprehensively characterized AMPK$^{\Delta}$ in its basal state and after in vitro phosphorylation using top-down mass spectrometry (MS), and assessed how phosphorylation of AMPK$^{\Delta}$ affects its activity. Unexpectedly, we found that bacterially-expressed AMPK$^{\Delta}$ was basally phosphorylated and localized the phosphorylation site to the His-tag. We found that AMPK$^{\Delta}$ had noticeable basal activity and was capable of phosphorylating itself and its substrates without activating phosphorylation at Thr172. Moreover, our data suggested that Thr172 is the only site phosphorylated by its upstream kinase, liver kinase B1, and that this phosphorylation dramatically increases the kinase activity of AMPK$^{\Delta}$. Importantly, we demonstrated that top-down MS in conjunction with in vitro phosphorylation assay is a powerful approach for monitoring phosphorylation reaction and determining sequential order of phosphorylation events in kinase-substrate systems.

Keywords: AMPK, Phosphorylation, Activity, Mass spectrometry, Electron capture dissociation

Received: 27 April 2015/Revised: 25 September 2015/Accepted: 26 September 2015/Published Online: 21 October 2015

Introduction

AMP-activated protein kinase (AMPK) is a highly conserved serine/threonine protein kinase that is essential in regulating energy metabolism in all eukaryotic cells [1–4]. It functions as an energy sensor by monitoring the energy status in the cell and serves as a master energy regulator that can turn on and off many metabolic pathways to regulate metabolism [3, 4]. AMPK is activated by elevation of the AMP:ATP ratio in response to stresses such as ischemia, hypoxia, and exercise [2, 5–8]. Once activated, AMPK modulates energy metabolism within the cell to restore homeostasis and promote cellular survival under conditions of stress [4, 9–12].

Structurally, AMPK is a heterotrimeric protein complex composed of a catalytic subunit (α) and two regulatory subunits (β and γ), with each subunit consisting of multiple isoforms encoded by different genes [13–15]. The α subunit plays an essential role in executing the function of the complex as a kinse. Two isoforms of the α subunit (α1 and α2) have been identified in mammalian cells, which possess a conserved N-terminal kinase domain and unique C-terminal tails containing the autoinhibitory and subunit binding domains [16–18]. In

Electronic supplementary material The online version of this article (doi:10.1007/s13361-015-1286-8) contains supplementary material, which is available to authorized users.

Correspondence to: Ying Ge; *e-mail:* ge2@wisc.edu

addition, both isoforms contain a conserved threonine residue (Thr172), located within the catalytic loop, the phosphorylation of which is considered to be essential for activation of the kinase [19]. Consequently, Thr172 phosphorylation is often used as an indicator of AMPK activation [20]. Previous studies have shown that C-terminal truncation of AMPKα at residue 312 abolishes binding of α subunit to the β and γ subunits, and yields a protein that is active upon canonical phosphorylation of Thr172, which is refered to as the AMPK catalytic domain and commonly used to substitute for the AMPK heterotrimeric complex in in vitro kinase assays [17, 21]. However, a comprehensive characterization of the AMPK catalytic domain is still lacking.

Top-down mass spectrometry (MS) has emerged as a powerful tool for the comprehensive characterization of various protein forms arising from genetic variations, alternative splicing, and post-translational modifications (PTMs) (collectively known as "proteoforms" [22]) [23–32]. We have previously shown that electron capture dissociation (ECD), one of the tandem mass spectrometry (MS/MS) techniques, is especially useful for mapping labile PTMs such as phosphorylation because they are well-preserved during the ECD fragmentation process [33–38]. Herein, we employed top-down MS to investigate the phosphorylation of truncated AMPKα with the aim of uncovering potential novel phosphorylation sites and understanding the role that phosphorylation plays in governing the activity of AMPKα. We expressed a His-tagged AMPK catalytic domain (denoted as $AMPK^{\Delta}$ hereafter) and have comprehensively characterized $AMPK^{\Delta}$ prior to and after in vitro phosphorylation by liver kinase B1 (LKB1). Surprisingly, we found that bacterially-expressed $AMPK^{\Delta}$ was, itself, phosphorylated at Ser18 in the His-tag sequence and was capable of phosphorylating itself and its substrates prior to incubation with LKB1, indicating that $AMPK^{\Delta}$ has noticeable basal activity in the absence of Thr172 phosphorylation. Additionally, we determined that Thr196 in our $AMPK^{\Delta}$ (equivalent to Thr172 in endogenous AMPKα) is the primary site phosphorylated by LKB1 and that the phosphorylation of this residue dramatically increases AMPK activity. Importantly, our approach combining top-down MS with in vitro phosphorylation assay enables the direct visualization of phosphorylation profile change over the course of in vitro incubation and highlights the utility of top-down MS for comprehensively characterizing protein phosphorylation.

Materials and Methods

Chemicals and Reagents

All reagents were purchased from Sigma Chemical Co. (St. Louis, MO, USA) unless noted otherwise. pET-28a (+) vector was purchased from EMD Chemicals (San Diego, CA, USA). Reverse transcriptase and GoTaq DNA polymerase were from Promega (Madison, WI, USA). The primers used for $AMPK^{\Delta}$ cloning were ordered from UW-Madison Biotechnology Center (Madison, WI, USA). Restriction enzymes and lambda protein phosphatase (λPP) were from New England Biolabs (Ipswich, MA, USA). T4 DNA Ligase was from Thermo Scientific (Waltham, MA, USA). Rosetta (DE3) competent *E. coli* cells, SAMS peptide, LKB1/STRAD/MO25 complex, 30 K molecular weight cutoff (MWCO) filters, and C18 ZipTip pipette tips were from Millipore (Billerica, MA, USA). Plasmid purification kit was from GeneTel Laboratories (Madison, WI, USA). Complete protease inhibitor cocktail was from Roche (Mannheim, Germany). AMPKα polyclonal antibody and AMPKα phospho-Thr172 polyclonal antibody were from Cell Signaling Technology (Beverly, MA, USA). Horseradish-conjugated anti-rabbit secondary antibody and Pierce ECL Western Blotting substrate were from Thermo Scientific (Waltham, MA, USA).

Cloning of Human $AMPK^{\Delta}$ for Bacterial Expression

cDNA for human AMPKα1 was obtained from reverse transcription of mRNA extracted from healthy human donor heart tissue. To clone human $AMPK^{\Delta}$, the coding sequence for the N-terminal 1-312 amino acids of AMPKα1 was generated by introducing two stop codons (TGATAG) after the codon of the 312th amino acid in the AMPKα1 sequence ($AMPK^{312}$). Primers used to amplify the coding sequence of $AMPK^{312}$ were custom-designed to include a restriction enzyme cutting site for NheI in the forward primer and a site for XhoI in the reverse primer for the ease of ligation. Following amplification of $AMPK^{312}$ by PCR, the DNA sequence for $AMPK^{312}$ was inserted into the pET-28a (+) expression vector using the NheI and XhoI sites. By this design, $AMPK^{312}$ was inserted downstream of the coding sequence for a 6xHis-tag ($AMPK^{\Delta}$ is used to denote His-tagged $AMPK^{312}$), which was used to facilitate purification of $AMPK^{\Delta}$.

Expression and Purification of Recombinant Human $AMPK^{\Delta}$

The $AMPK^{\Delta}$ construct was transformed into Rossetta (DE3) competent *E. coli* cells and the transformants were selected on LB agar plates containing 50 μg/mL kanamycin. Plasmids from inoculated single colonies were extracted to confirm the successful insertion of the $AMPK^{\Delta}$ coding sequence by PCR and DNA sequencing and those containing the correct insert sequence were used for protein expression. For large-scale protein expression, 1 L of LB broth supplemented with 50 μg/mL kanamycin was inoculated with 50 mL of overnight culture and grown in the incubator at 37°C until an OD600 of 0.6–0.8 was reached. Protein expression was induced by adding 0.1 mM IPTG and shaking at 225 rpm and 30°C for 6 h. Cells were pelleted by centrifugation and lysed by sonication. Insoluble material was removed by centrifugation at 7500 for 20 min at 4°C and the supernatant was used for subsequent protein purification [39]. Purification was conducted at 4°C using Profinity immobilized metal affinity chromatography (IMAC) Ni-charged resin (BioRad, Hercules, CA, USA) following the manufacturer's instructions. The concentration and

purity of recombinant AMPK$^{\Delta}$ were assessed by sodium dodecyl sulfate-polyacrylamide gel electrophoresis (SDS-PAGE). The IMAC purified AMPK$^{\Delta}$ was desalted with a 30 K MWCO filter by 0.1% formic acid. After elution, samples were mixed with 45% methanol and 5% acetic acid and analyzed by top-down MS.

In Vitro Phosphorylation of AMPK$^{\Delta}$

Purified recombinant AMPK$^{\Delta}$ protein (10 μM) was incubated with the LKB1/Ste20-related adaptor (STRAD)/mouse protein 25(MO25) complex (100 nM) with a substrate-to-enzyme ratio of 100:1 in 100 μL kinase buffer (50 mM HEPES pH 7.4, 5 mM $MgCl_2$, 1 mM $CaCl_2$, 2 mM DTT, 200 μM ATP, and protease inhibitor cocktail) at 30°C for 5, 10, and 30 min [40]. The reaction was stopped by freezing the samples at –80°C. In vitro phosphorylated AMPK$^{\Delta}$ was further desalted using MWCO filter and then analyzed using top-down MS as described below to identify sites of phosphorylation by LKB1/STRAD/MO25. To quantify the change in AMPK$^{\Delta}$ phosphorylation after in vitro phosphorylation by LKB1, the relative percentages of all unphosphorylated and phosphorylated proteoforms, as well as the total phosphorylation level, were calculated as previously described [38].

Dephosphorylation and Autophosphorylation of AMPK$^{\Delta}$

To determine if bacterially expressed AMPK$^{\Delta}$ is capable of phosphorylating itself, purified recombinant AMPK$^{\Delta}$ (100 μg) protein was incubated with lambda protein phosphatase (λPP) in 1× protein metallophosphatase buffer supplemented with 1 mM $MnCl_2$ at 30°C for 1 h; λPP-treated AMPK$^{\Delta}$ was then inactivated at 65°C for 1 h, cleaned with 30 K MWCO (to remove λPP, which has molecular mass of 25 kDa) and then incubated with 400 μM ATP in kinase buffer at 30°C for 1 h; purified recombinant AMPK$^{\Delta}$, λPP-treated AMPK$^{\Delta}$, and ATP-incubated AMPK$^{\Delta}$ that has been treated with λPP were then further desalted using 30 K MWCO filter and analyzed using top-down MS.

In Vitro Phosphorylation of SAMS Peptide

To assess the activity of in vitro-phosphorylated AMPK$^{\Delta}$ as well as bacterially-expressed AMPK$^{\Delta}$, 200 μM SAMS peptide was incubated with 2 μM AMPK (incubated with LKB1/STRAD/MO25 for 0, 5, 10, and 30 min) in kinase buffer for 10 min at 30°C. The reaction was stopped by heating the sample to 95°C for 5 min. The samples were then desalted using C18 ZipTip pipette tips following the manufacturer's instructions. After elution, the desalted peptides were subjected to MS analysis.

Top-Down MS Analysis

A 7 T linear ion trap/Fourier transform ion cyclotron resonance (FT-ICR) mass spectrometer (LTQ/FT Ultra, Thermo Scientific, Bremen, Germany) was used to analyze recombinant AMPK$^{\Delta}$ and SAMS peptide. The sample was introduced into the mass spectrometer using an automated chip-based nanoelectrospray ionization (ESI) source (Triversa NanoMate, Advion Bioscience, Ithaca, NY, USA) similarly as described previously [41]. For full MS analysis of AMPK$^{\Delta}$, the resolving power of the FT-ICR was typically set at 200,000 whereas a resolution of 100,000 was used for the analysis of SAMS peptide. For MS/MS analysis, the precursor molecular ions at individual charge states were first isolated in the gas phase and then fragmented using 12%–20% normalized collision energy for collisionally activated dissociation (CAD) or 2.5-3.5% electron energy for ECD (corresponding to 1.3 to 2.3 eV) with a 70 ms duration and no additional delay [41].

In-house developed MASH Suite software, which uses a modified version of the THRASH algorithm, was used to analyze the MS and MS/MS spectra generated for AMPK$^{\Delta}$ [42]. The peaks were extracted with a setting of signal-to-noise ratio threshold of 3 and a minimum fit of 60% and then individual peaks were manually validated before uploading the DNA-predicted amino acid sequence for AMPK$^{\Delta}$. Fragment ions were assigned by matching the experimentally-determined molecular mass with those calculated for theoretical fragments with a mass tolerance of 10 ppm. For the identification of intact AMPK$^{\Delta}$, allowance for N-terminal Met removal was made. For the fragment ions containing possible phosphorylation sites, a mass shift of approximately 80 Da was manually validated to confirm or exclude the presence of phosphorylation. The reported molecular mass given for intact proteins and fragment ions corresponds to the most abundant and monoisotopic molecular mass, respectively [41].

Western Blot

Western blot analysis using an AMPKα antibody was used to confirm AMPK expression and purification using the IMAC Ni-charged column. A phosphor-AMPKα (Thr172) antibody was used to analyze Thr172 phosphorylation following incubation with LKB1/STRAD/MO25 complex for 0 min (no kinase added), 5 min, 10 min, and 30 min. After separation by 12.5% SDS-PAGE, the protein samples were transferred to a PVDF membrane using a semi-dry blotter (Thermo Scientific) at 25 V for 40 min. The membrane was blocked with 5% non-fat milk in TBST at room temperature for 3 h. The membrane was then washed and subsequently incubated with primary antibody (AMPKα or pThr172-AMPKα antibody) diluted 1:4000 on a shaker at 4°C for overnight. After incubation with the primary antibody, the blot was washed, incubated with horseradish peroxidase conjugated secondary antibody at room temperature for 1 h, washed, and developed using Pierce ECL substrate.

Results

AMPK$^{\Delta}$ Cloning, Expression, Purification, and MS Analysis

The catalytic domain of AMPK is reported to be composed of the first 312 amino acids in the α subunit [17]. To study the

phosphorylation and activity of the catalytic domain of AMPKα subunit, a construct was made by inserting the coding sequence of the first 312 amino acids in the AMPKα1 subunit to the downstream of a His-tag coding sequence in pET-28a(+) vector to express AMPK$^{\Delta}$ (Figure 1a). SDS-PAGE analysis was used to assess the protein concentration of affinity-purified AMPK$^{\Delta}$ in the IMAC eluent (Figure 1b). The expression of AMPK$^{\Delta}$ was further confirmed by Western blotting using AMPKα antibody (Supplemental Figure S1).

High-resolution MS analysis of bacterially-expressed AMPK$^{\Delta}$ revealed a complex spectrum with multiple peaks, indicating the existence of multiple AMPK$^{\Delta}$ proteoforms in the sample (Figure 1c). Of all the proteoforms detected by MS, none displayed a molecular mass that matches the theoretical molecular mass of AMPK$^{\Delta}$ calculated based on the DNA sequence from the construct. The experimental molecular mass of the most abundant proteoform was 37,873.30 Da, which is 131.20 Da less than the calculated molecular mass of AMPK$^{\Delta}$. This is presumably due to the removal of the N-terminal Met, which is very common among endogenous and recombinant proteins. The experimental molecular mass matched well with the calculated molecular mass of AMPK$^{\Delta}$ without the N-terminal Met (2.1 ppm). The precursor ions (M^{35+}) of this proteoform were isolated in the gas phase and subsequently fragmented by ECD and CAD to confirm the sequence of AMPK$^{\Delta}$. The observation that no N-terminal fragments (***b*** and ***c*** ions) could be identified using the sequence containing the N-terminal Met, whereas significantly more N-terminal fragments were identified using the sequence without the N-terminal Met, confirmed that the N-terminal Met of bacterially-expressed AMPK$^{\Delta}$ was indeed removed.

Interestingly, we observed that the molecular mass of AMPK$^{\Delta}$ (37869.24 Da) was approximately 4 Da less than the theoretical molecular mass (37,873.30 Da) when no DTT was added over the course of protein purification (Supplemental Figure S2). We reasoned that this was likely caused by the formation of two disulfide bonds (S–S, the formation of one disulfide bond results in about 2 Da mass decrease), as adding more than 5 mM DTT completely prevented this from occurring. We have located the position of the two disulfide bonds in AMPK$^{\Delta}$ using MS/MS: one S–S bond is formed between Cys154 and Cys198 and the other is formed between two of three Cys residues (Cys321, Cys326, and Cys334) (Supplemental Figures S3 and S4, Supplemental Results).

Mapping the Phosphorylation Site in Basally Mono-Phosphorylated AMPK$^{\Delta}$ (pAMPK$^{\Delta}$)

Surprisingly, of all the AMPK$^{\Delta}$ proteoforms observed in the spectrum for AMPK$^{\Delta}$ directly purified from *E. coli*, the second most abundant proteoform had an experimental molecular mass of 37,953.26 Da, which is 79.96 Da larger than that of unmodified AMPK$^{\Delta}$ (Figure 1c). Thus, this proteoform presumably corresponds to a *p*AMPK$^{\Delta}$ (mass increase of 79.96 Da per phosphorylation). To locate the phosphorylation site, the precursor ions of *p*AMPK$^{\Delta}$ with the experimental molecular

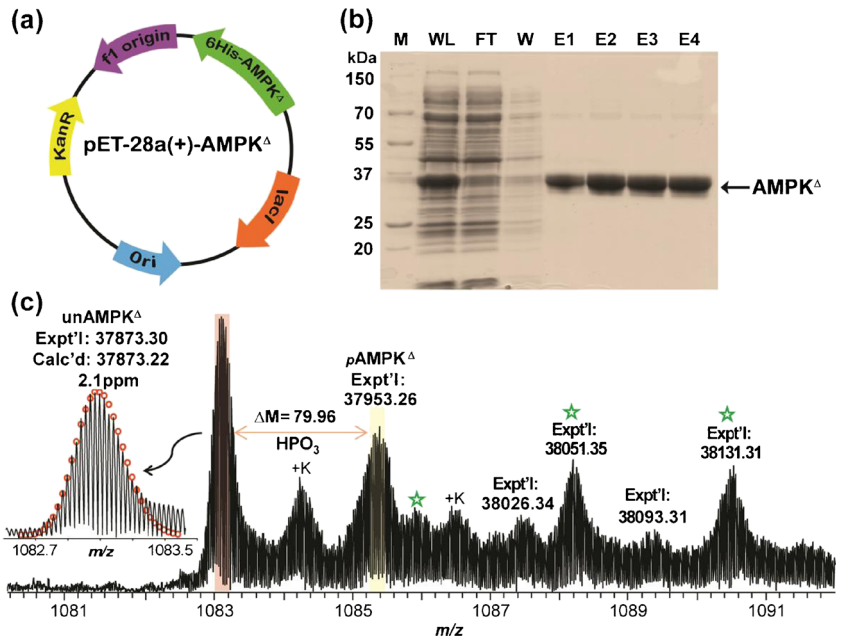

Figure 1. AMPK$^{\Delta}$ cloning, purification, and MS analysis. (**a**) Construction of pET-28a(+)- AMPK$^{\Delta}$ expression plasmid. (**b**) SDS-PAGE analysis of AMPK$^{\Delta}$ affinity-purified using a nickel-charged IMAC column. M, molecular weight marker; WL, whole lysate; FT, flow-through; W, wash; E, elution. (**c**) MS analysis of bacterially-expressed AMPK$^{\Delta}$. The spectrum is a zoom-in view of a single charge state, M^{35+}. unAMPK$^{\Delta}$ = unphosphorylated AMPK$^{\Delta}$; *p*AMPK$^{\Delta}$ = mono-phosphorylated AMPK$^{\Delta}$. Inset, isotopically resolved molecular ion of AMPK$^{\Delta}$ with high-accuracy molecular mass measurement. Circles, the theoretical isotopic abundance distribution of the isotopomer peaks corresponding to the assigned mass. Calc'd = calculated most abundant mass; Expt'l = experimental most abundant mass. +K = potassium adduct (+38 Da); star indicates noncovalent phosphate adduct

mass of 37593.26 Da (Figure 2a) were isolated and fragmented using ECD and CAD. Fragment ions from CAD and ECD were assigned to fragments expected based on the unmodified sequence of AMPK$^{\Delta}$ without the N-terminal Met (Figure 2b). A total of 47 ***b*** ions and 41 ***y*** ions were detected in three combined CAD spectra of the basally *p*AMPK$^{\Delta}$. The ***b*** ions detected were all generated from cleavage C-terminal to Asp32 and were 79.96 Da larger than their corresponding calculated molecular

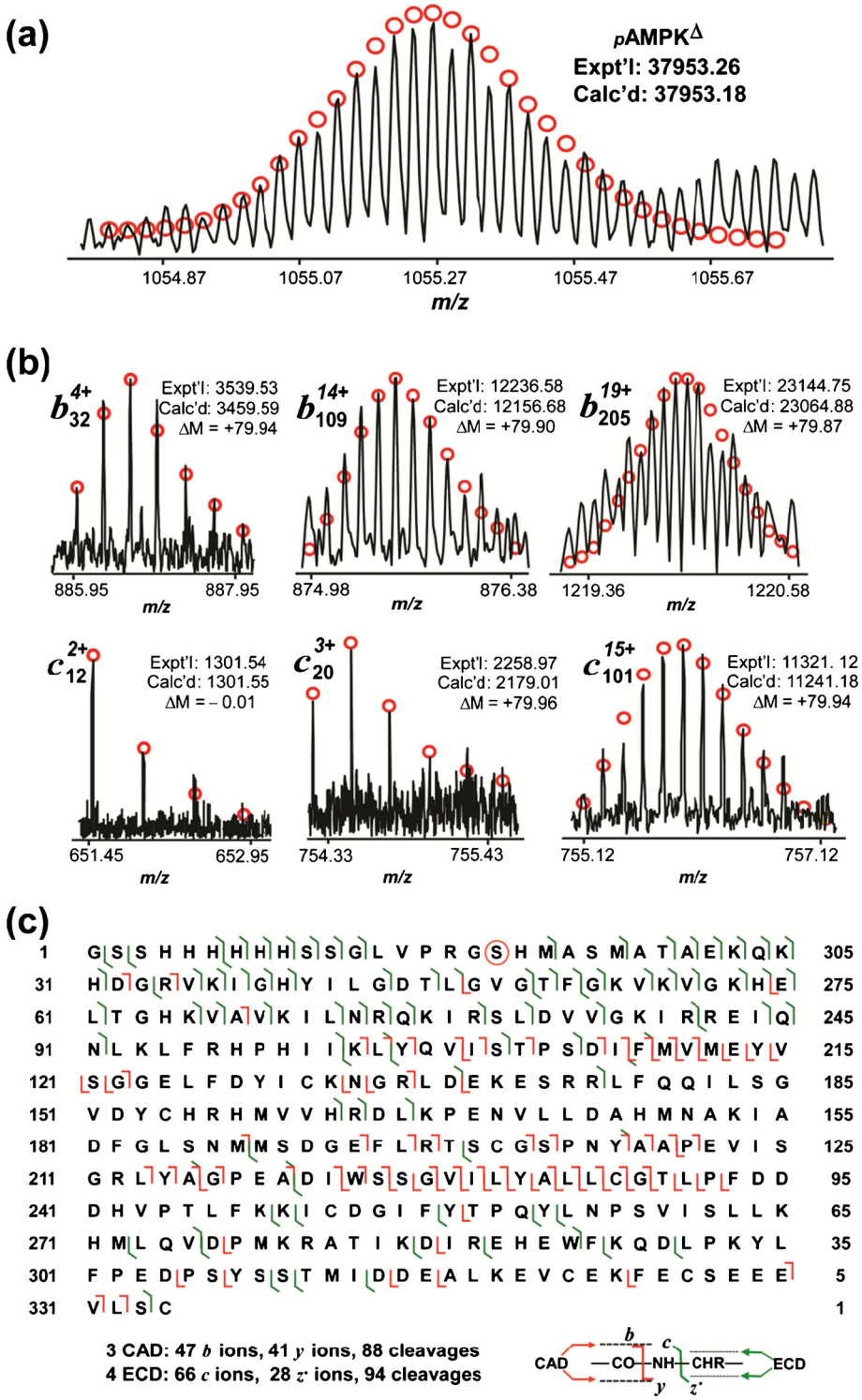

Figure 2. Top-down MS characterization of basally *p*AMPK$^{\Delta}$. (**a**) High-accuracy mass measurement of basally *p*AMPK$^{\Delta}$. (**b**) Representative fragment ions from basally *p*AMPK$^{\Delta}$. (**c**) MS/MS fragmentation and product ion map from CAD and ECD for basally *p*AMPK$^{\Delta}$. Circle in the sequence indicates the location of the phosphorylation site identified by MS/MS analysis. Calc'd = calculated molecular mass; Expt'l = experimental molecular mass

mass, revealing that the mass discrepancy of 79.96 Da arose from modification of a residue N-terminal to Asp32 in the sequence; 66 ***c*** ions and 28 ***z*·** ions in total were detected in four combined ECD spectra; 7 ***c*** ions from c_6 to c_{12} were detected without mass discrepancy compared with their predicted ions, whereas c_{20} was the first ***c*** ions detected with a mass increase of 79.96 Da. Similarly, all ***c*** ions generated C-terminal to c_{20} bore this mass increase, demonstrating that the site of phosphorylation was located between Leu13 and Met20. As Ser18 is the only residue that can be phosphorylated in the eight residues between Leu13 and Met20, the site of phosphorylation in basally *p*AMPK$^{\Delta}$ was confidently localized to Ser18, which is located within the His-tag sequence (Figure 2c).

Given that the adjacent sequence of Ser18 (LVPRGS) in AMPK$^{\Delta}$ lies in the well-demonstrated phosphor-AMPK substrate motif sequence (LXRX/RXS) [43], we reason that the phosphorylation of Ser18 in bacterially expressed AMPK$^{\Delta}$ is likely the product of autophosphorylation. To determine if AMPK$^{\Delta}$ is capable of phosphorylating itself, we incubated λPP-treated AMPK$^{\Delta}$ with ATP in kinase buffer and found that dephosphorylated AMPK$^{\Delta}$ became re-phosphorylated (Supplemental Results, Supplemental Figure S5), which strongly suggests that AMPK$^{\Delta}$ is indeed capable of phosphorylating itself (autophosphorylation). Thus, it appears very likely that the phosphorylation of Ser18 in basally *p*AMPK$^{\Delta}$ is autophosphorylated, although we cannot rule out the possibility that *E. coli* does express kinases that could potentially phosphorylate Ser18 in AMPK$^{\Delta}$.

In Vitro Phosphorylation of AMPK$^{\Delta}$

LKB1 is a well-known upstream kinase for AMPK and phosphorylation of Thr172 in AMPKα by LKB1 is predominantly responsible for AMPK activation in the cell [44–46]. To investigate if there are other potential sites phosphorylated by LKB1, we incubated AMPK$^{\Delta}$ with the LKB1/STRAD/MO25 complex for 5, 10, and 30 min, and monitored changes in AMPK$^{\Delta}$ phosphorylation using MS (Figure 3a). In contrast to the basal AMPK$^{\Delta}$ (purified from *E. coli* without activation), where the most abundant proteoform was unmodified AMPK$^{\Delta}$, *p*AMPK$^{\Delta}$ was the most abundant proteoform detected after 5 min incubation with the LKB1/STRAD/MO25 complex. Bis-phosphorylated AMPK$^{\Delta}$ (*pp*AMPK$^{\Delta}$) became most prominent after 10 min incubation, whereas tris-phosphorylated AMPK$^{\Delta}$ (*ppp*AMPK$^{\Delta}$) emerged as the dominating peak after 30 min incubation with the LKB1/STRAD/MO25 complex. Further incubation of AMPK$^{\Delta}$ with LKB1/STRAD/MO25 for longer durations did not change the phosphorylation profile,

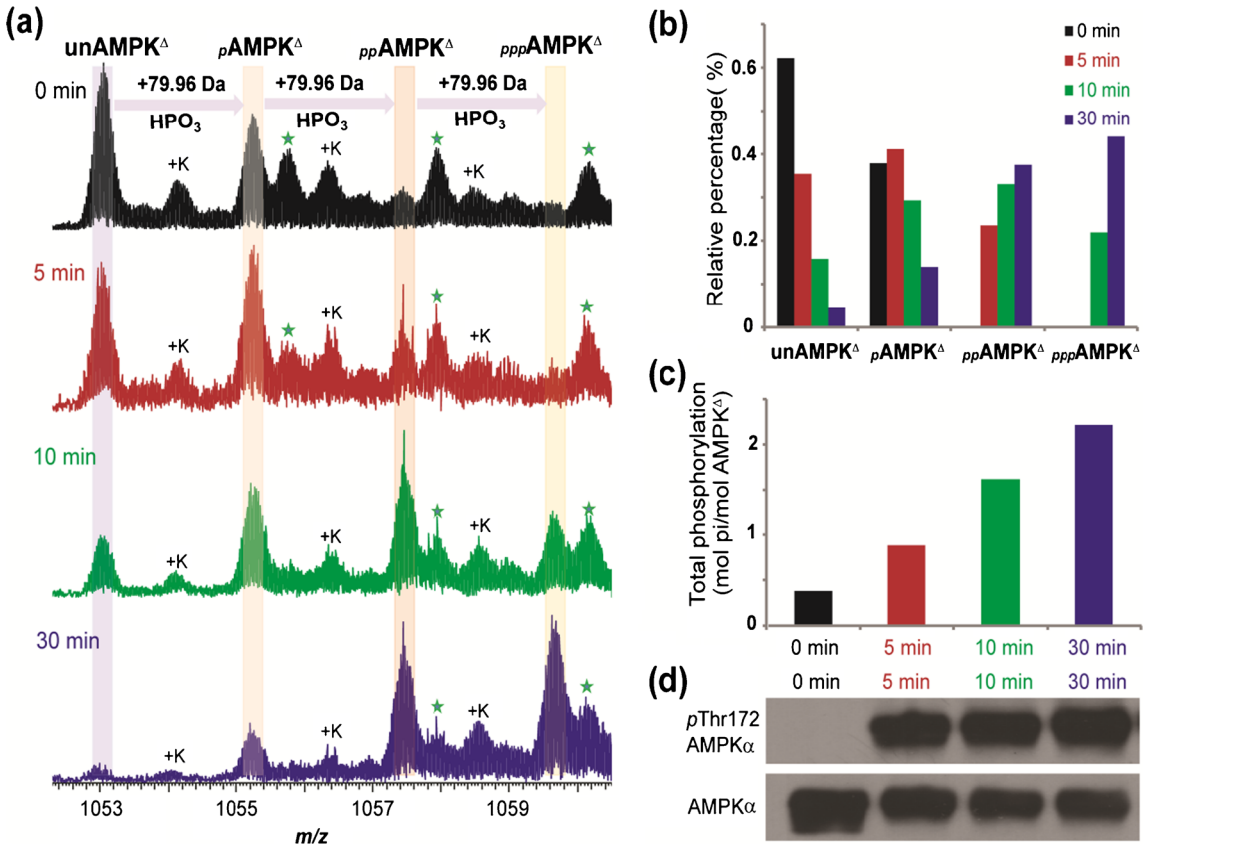

Figure 3. MS analysis of in vitro-phosphorylated AMPK$^{\Delta}$. (**a**) High-resolution MS spectra of AMPK$^{\Delta}$ that was incubated with the LKB1/MO25/STRAD complex for 0 min (basal), 5 min, 10 min, and 30 min, respectively. +K = potassium adduct (+38 Da); star indicates noncovalent phosphate adduct. (**b**) Change of relative percentage of unAMPK$^{\Delta}$, *p*AMPK$^{\Delta}$, *pp*AMPK$^{\Delta}$, and *ppp*AMPK$^{\Delta}$ over the course of incubation with the LKB1/MO25/STRAD complex at selective time points; (**c**) The total amount of phosphorylation in AMPK$^{\Delta}$ at selective incubation durations. (**d**) Western blot analysis of Thr172 phosphorylation following in vitro phosphorylation

with *ppp*AMPK$^{\Delta}$ remaining to be the most abundant proteoform for all subsequent durations. In addition to phosphorylated AMPK$^{\Delta}$ proteoforms, multiple noncovalent potassium and phosphate adducts were also observed in the spectra. Quantitative analysis of the observed phosphorylated proteoforms showed that the relative percentage of unphosphorylated AMPK$^{\Delta}$ decreased over the course of incubation whereas *pp*AMPK$^{\Delta}$ and *ppp*AMPK$^{\Delta}$ gradually became the dominant proteoforms in the mixture (Figure 3b). Consistent with the increase in the relative abundance of *pp*AMPK$^{\Delta}$ and *ppp*AMPK$^{\Delta}$, the total phosphorylation of AMPK$^{\Delta}$ increased with prolonged incubation time, suggesting phosphorylation of AMPK$^{\Delta}$ by LKB1/STRAD/MO25 (Figure 3c). Since LKB1/STRAD/MO25 is known to phosphorylate endogenous AMPK at Thr172, to confirm LKB1/STRAD/MO25-meditated phosphorylation of AMPK$^{\Delta}$ we conducted Western blotting to determine whether in vitro phosphorylated AMPK$^{\Delta}$ was phosphorylated at Thr172. Expectedly, AMPK$^{\Delta}$ that had been incubated with LKB1/STRAD/MO25 (5, 10, and 30 min) was phosphorylated at Thr172, whereas bacterially-purified AMPK$^{\Delta}$ that was not incubated with LKB1/STRAD/MO25 was not phosphorylated at Thr172 (Figure 3d).

Top-Down MS Characterization of In Vitro Phosphorylated AMPK$^{\Delta}$

To locate the phosphorylation site in the *p*AMPK$^{\Delta}$ from the in vitro phosphorylation assay, the precursor ions with experimental molecular mass of 37953.18 Da from 5 min in vitro phosphorylation were isolated and dissociated by both CAD and ECD, respectively (Figure 4). The fact that a mixture of un- and mono-phosphorylated $\boldsymbol{b}$ and $\boldsymbol{c}$ ions coexisted in CAD and ECD (Supplemental Figure S6) suggested partial phosphorylation occupancy in *p*AMPK$^{\Delta}$ after 5 min in vitro phosphorylation [33, 47]. The presence of unphosphorylated and phosphorylated pairs of $\boldsymbol{c}_{26}$ and $\boldsymbol{c}_{101}$ ions indicated that some protein positional isomers (i.e., the proteoforms that have the same functional groups but differ from each other in the location of the functional groups) have a phosphorylation site N-terminal to residue 26 and that another is phosphorylated C-terminal to residue 101. Of all the fragment ions detected in ECD experiment, 5 $\boldsymbol{c}$ ions generated N-terminal to Leu13 were detected without mass discrepancy from their calculated molecular mass, whereas 16 $\boldsymbol{c}$ ions from $\boldsymbol{c}_{18}$ to $\boldsymbol{c}_{185}$ were detected with an 80 Da mass increase, suggesting a phosphorylation site exists between Leu13 and Ser18 in some of the *p*AMPK$^{\Delta}$. As Ser18 is the only residue in this region that can be phosphorylated, Ser18 was unambiguously identified as one of the phosphorylation sites in *p*AMPK$^{\Delta}$. For the identification of other phosphorylation sites in *p*AMPK$^{\Delta}$, the detection of $\boldsymbol{z}^{\cdot}_{115}$ as the biggest unphosphorylated C-terminal fragment and $\boldsymbol{y}_{214}$ as the smallest phosphorylated C-terminal fragment indicated a phosphorylation site between Ser121 and Asp220. Lack of fragments between Ser121 and Asp220 rendered it difficult to further locate the phosphorylation site. However, based on the observation that AMPK$^{\Delta}$ incubated with LKB1/STRAD/MO25 for 5 min was found phosphorylated at Thr172 by Western blot analysis (Figure 3d), together with findings from numerous studies showing that Thr172 is the primary site phosphorylated by LKB1, we reasoned that Thr196 in our His-tagged AMPK$^{\Delta}$ (which is equivalent to Thr172 in endogenous AMPK) is another site of phosphorylation in *p*AMPK$^{\Delta}$. Overall, our MS/MS and Western blot data confirmed phosphorylation at Ser18 and Thr196 in *p*AMPK$^{\Delta}$ incubated with LKB1/STRAD/MO25 for 5 min, although it should be noted that the existence of other phosphorylation sites between Ser121 and Asp220 cannot be ruled out because of poor sequence coverage in this region (Supplemental Figure S7).

To map the phosphorylation sites in *pp*AMPK$^{\Delta}$, the precursor ions with experimental molecular mass of 38033.14 Da in AMPK$^{\Delta}$ incubated with LKB1/STRAD/MO25 for 10 min were isolated and subjected to ECD (Supplemental Figure S8). Two ECD experiments generated 67 $\boldsymbol{c}$ ions and 10 $\boldsymbol{z}^{\cdot}$ ions. The observation that the largest unphosphorylated $\boldsymbol{c}$ ion detected was $\boldsymbol{c}_{12}$ and the smallest mono-phosphorylated $\boldsymbol{c}$ ion was $\boldsymbol{c}_{19}$ unambiguously nailed down to one site of phosphorylation to Ser18. Based on the fact that $\boldsymbol{c}_{136}$ was the largest mono-phosphorylated ion detected, as well as the fact that $\boldsymbol{z}^{\cdot}_{119}$ was the largest C-terminal unphosphorylated fragment detected, we concluded that the other phosphorylation site must be located between Glu137 and Ala215. Thus, for the same reason as stated above, Thr196 (equivalent to Thr172 in endogenous AMPK) was deduced to be the other phosphorylation site in *pp*AMPK$^{\Delta}$. Thus, Ser18 and Thr196 were the two phosphorylated residues in *pp*AMPK$^{\Delta}$.

To characterize *ppp*AMPK$^{\Delta}$, precursor ions corresponding to *ppp*AMPK$^{\Delta}$ (experimental molecular mass: 38113.12 Da) were isolated and fragmented using CAD and ECD (Figure 5). Of the $\boldsymbol{b}$ ions we mapped from the CAD experiments, 17 $\boldsymbol{b}$ ions from $\boldsymbol{b}_{32}$ to $\boldsymbol{b}_{187}$ were detected as bis-phosphorylated fragments and 24 $\boldsymbol{b}$ ions from $\boldsymbol{b}_{200}$ to $\boldsymbol{b}_{332}$ were detected as tris-phosphorylated fragments, suggesting that two phosphorylation sites were located N-terminal to Gly33 and that one phosphorylation site existed in the region between Met187 and Ser200. In our ECD experiments, $\boldsymbol{c}_{12}$ was detected as unphosphorylated fragment, whereas $\boldsymbol{c}_{23}$ was detected as the first bis-phosphorylated fragment, providing definitive evidence that Ser18 and Ser22 were two phosphorylated residues as they are the only two residues between Leu13 and Met23 that can be phosphorylated. Despite the fact that no other fragments were detected in the region between Met187 and Ser200, our Western blot results unambiguously confirmed phosphorylation at Thr172 of AMPKα, which is equivalent to Thr196 in our AMPK$^{\Delta}$, after incubation with LKB1/STRAD/MO25 for 30 min (Figure 3d). Taken together, Ser18 and Ser22 in the His-tag region as well as Thr196 in the sequence of the AMPK catalytic domain are the three phosphorylation sites in *ppp*AMPK$^{\Delta}$.

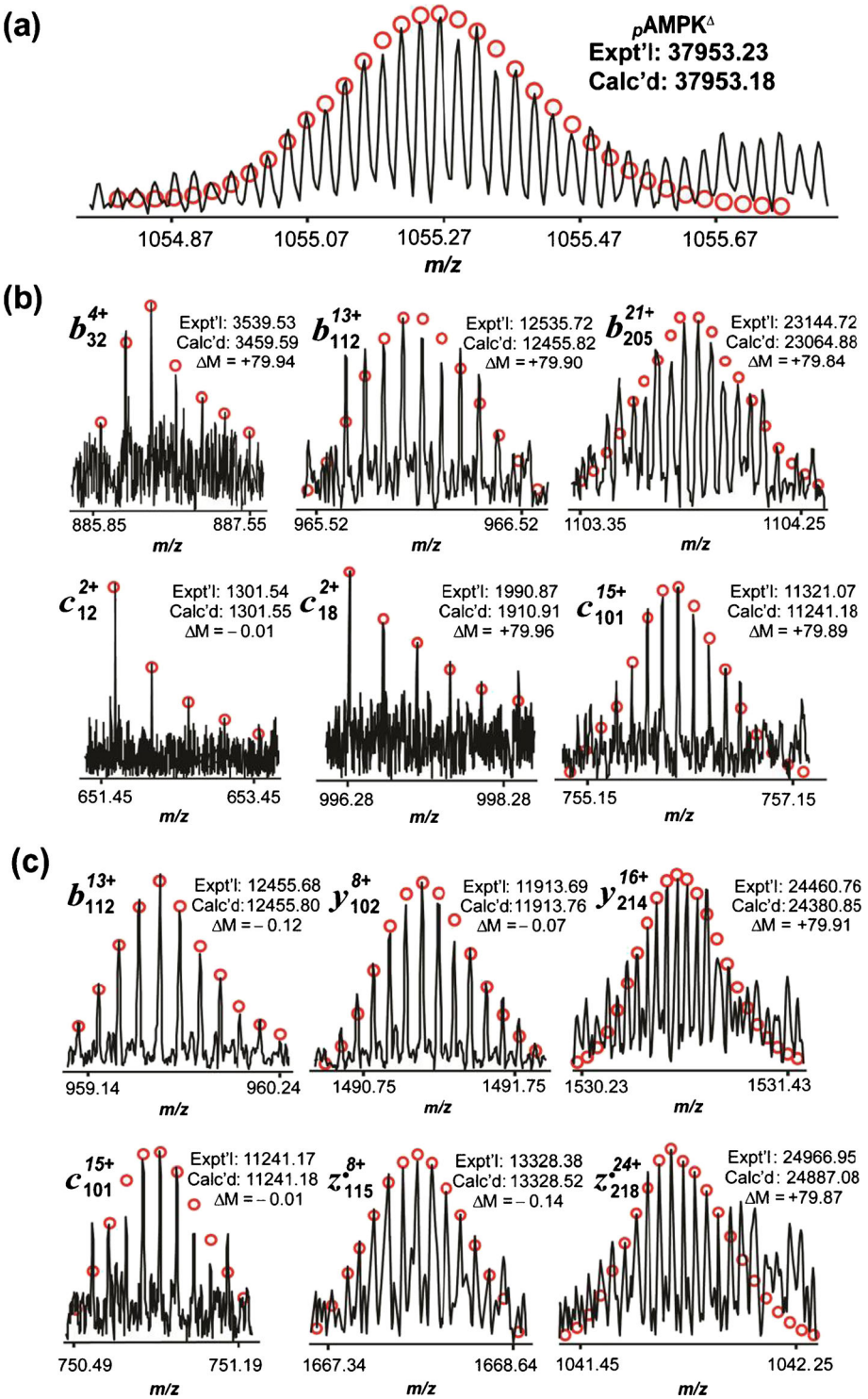

Figure 4. MS characterization of $_p$AMPK$^\Delta$ after 5 min of in vitro phosphorylation by LKB1/MO25/STRAD complex. (**a**) High-accuracy mass measurement of $_p$AMPK$^\Delta$. (**b**) Representative fragment ions for $_p$AMPK$^\Delta$ confirming phosphorylation at Ser 18. (**c**) Representative fragment ions for $_p$AMPK$^\Delta$ suggesting a phosphorylation site at Thr196, which is equivalent to Thr172 in endogenous AMPK

Assessment of Activity of AMPK$^\Delta$ in Relation to Its Phosphorylation States

To investigate how phosphorylation affects the catalytic activity of AMPK$^\Delta$, we incubated a well-known AMPK substrate, SAMS peptide, with basal AMPK$^\Delta$ (purified from *E. coli* without activation) as well as AMPK$^\Delta$ that had been activated by LKB1/STRAD/MO25 for 5, 10, 30, min incubations, respectively, and assessed to what extent these various forms of

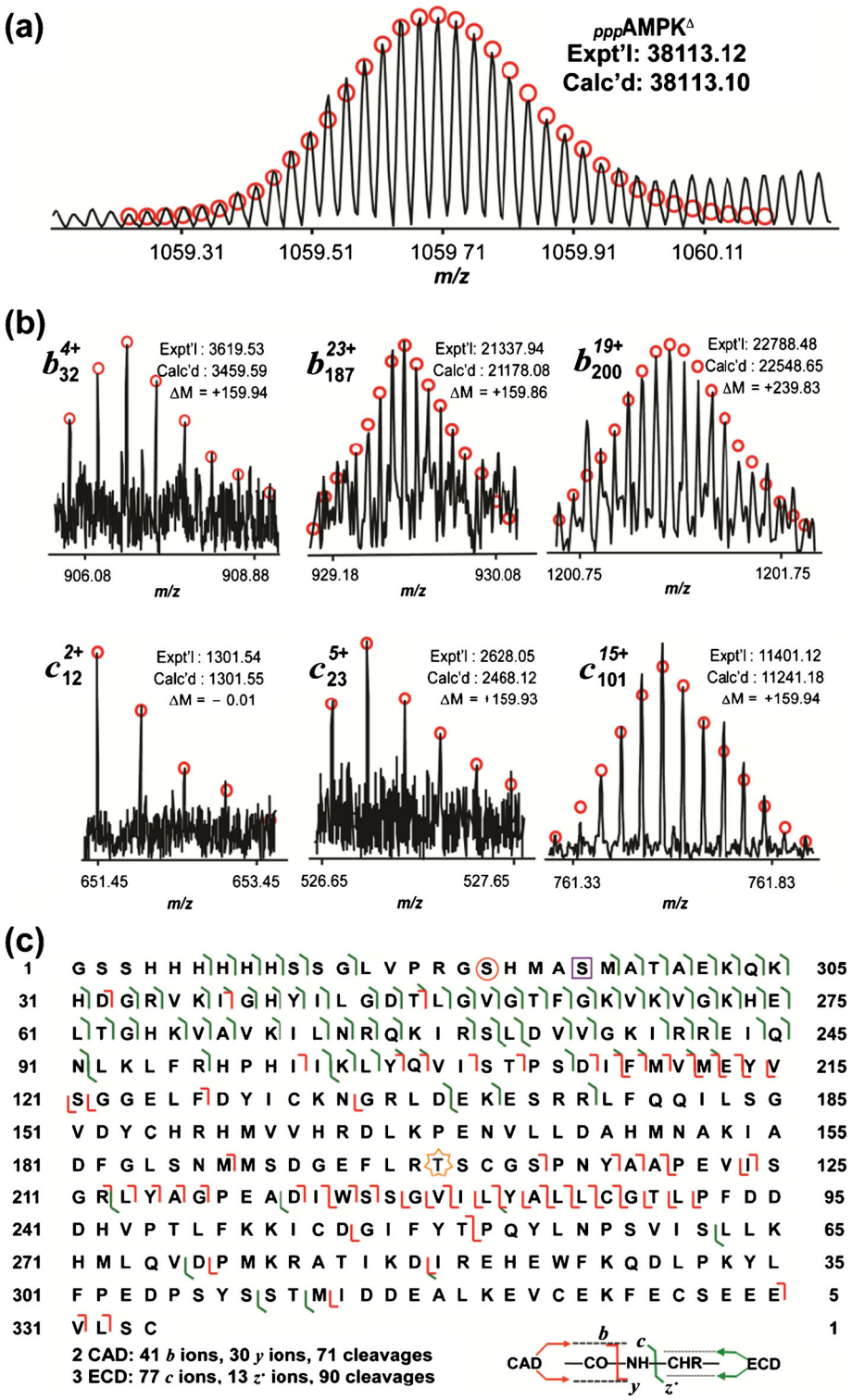

Figure 5. MS characterization of $_{ppp}$AMPK$^{\Delta}$ after 30 min of in vitro phosphorylation by LKB1/MO25/STRAD complex. (**a**) High-accuracy mass measurement of $_{ppp}$AMPK$^{\Delta}$. (**b**) Representative fragment ions from $_{ppp}$AMPK$^{\Delta}$. (**c**) MS/MS fragmentation and product ion map from CAD and ECD for $_{ppp}$AMPK$^{\Delta}$. Circle and square indicate that Ser18 and Ser22 are two distinct phosphorylation sites identified from MS/MS data; star suggests that Thr196 is another phosphorylation site in $_{ppp}$AMPK$^{\Delta}$

phosphorylated AMPK can phosphorylate SAMS peptide (Figure 6, Supplemental Figure S9). A brief incubation (10 min) of SAMS peptide with activated AMPK$^{\Delta}$ (incubated 5 min with LKB1/STRAD/MO25) rendered SAMS peptide completely phosphorylated (Supplemental Figure S9), which indicates that AMPK$^{\Delta}$ had been activated by 5 min

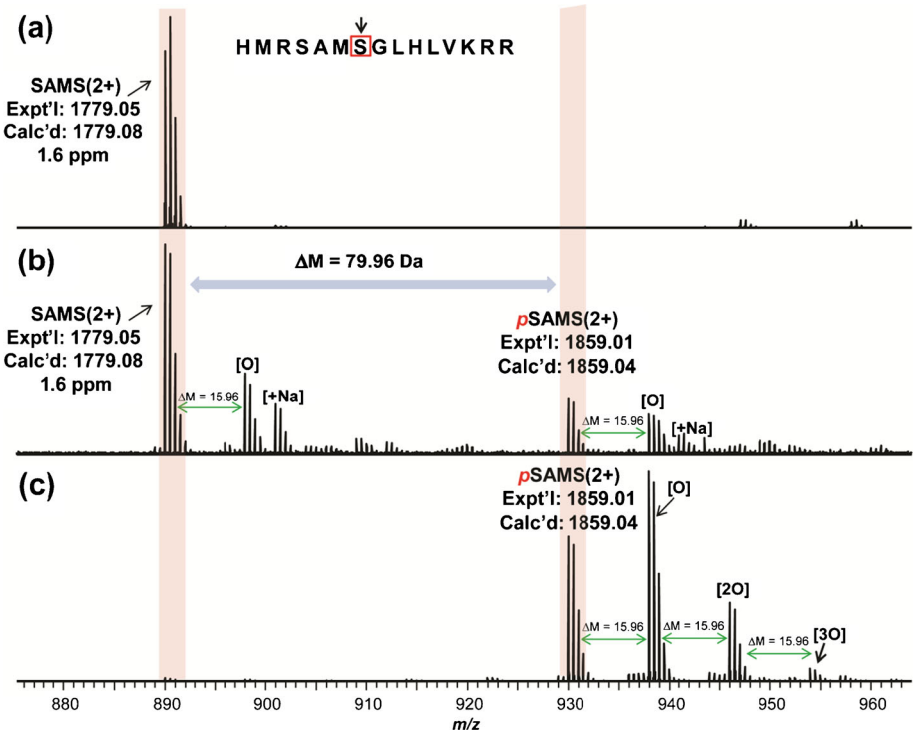

Figure 6. MS spectra of SAMS peptide before and after phosphorylation by AMPK$^{\Delta}$. (**a**) Pure SAMS peptide. (**b**) SAMS peptide after 10 min incubation with basal AMPK$^{\Delta}$ purified from *E. coli* without activation by LKB1/STRAD/MO25. **(c)** SAMS peptide after 10 min incubation with AMPK$^{\Delta}$ that had been activated by LKB1/STRAD/MO25 for 5 min. *p* = phosphorylation; O = oxidation (+16 Da); +Na, = sodium adduct (+22 Da). The sequence of the SAMS peptide is shown as inset in **(a)** with the phosphorylated Ser highlighted in square and indicated by the arrow

incubation with LKB1/STRAD/MO25. Both un- and mono-phosphorylated SAMS peptides were detected when SAMS peptide was incubated with purified AMPK$^{\Delta}$ that was not incubated with the LKB1/STRAD/MO25 complex, demonstrating that the basal AMPK$^{\Delta}$ could still phosphorylate SAMS peptide and, thus, confirming that it indeed has basal activity (Figure 6). Taken together, our data implies that AMPK$^{\Delta}$ requires phosphorylation at Thr172 catalyzed by its upstream kinase to gain full activity; however, this phosphorylation is not an absolute requirement for its basal catalytic activity.

Discussion

AMPKα Phosphorylation and Catalytic Activity

AMPK is the master regulator of energy metabolism and plays important roles in many biological process [1–4]; however, the mechanistic details on the phosphorylation state and the activity of AMPK remain inconclusive. Although Thr172 has been shown to be the major phosphorylation site regulating the activity of the AMPK complex as well as truncated α subunits [17, 19, 21], whether there are other phosphorylation sites involved in fine-tuning the activity of AMPK remains uncertain. Stein et al. showed that phosphatase treatment of an AMPK T172D mutant, which mimics the phosphorylation of Thr172, led to decreased activity compared with wild-type AMPK, suggesting that other phosphorylation sites are involved in regulating AMPK activity [21]. Furthermore, Woods et al. identified two more phosphorylation sites (Thr258 and Ser485), in addition to Thr172, in the α subunits from both endogenous and recombinant AMPK complex; however, these sites do not appear to play a significant role in regulating the activity of AMPK [48].

Since AMPK catalytic domain is commonly used to substitute for the AMPK heterotrimeric complex in in vitro kinase assays, we utilized top-down mass spectrometry to comprehensively characterize the phosphorylation in AMPK$^{\Delta}$. We detected three phosphorylation sites in our recombinant AMPK$^{\Delta}$ following incubation with its upstream kinase LKB1; two phosphorylation sites (Ser18 and Ser22) are located in the His-tag region which lack biologically relevance; Thr172 is the only phosphorylation site with biological significance detected in the in vitro phosphorylated AMPK$^{\Delta}$. Our finding that Thr172 is the only phosphorylation site in the in vitro phosphorylated AMPK$^{\Delta}$ reveals that phosphorylation of Thr172 is primarily responsible for the activation of the catalytic domain of AMPKα, which is consistent with the findings of previous studies using radiolabeled [γ-^{32}P] ATP-based assay [17, 40]. Moreover, the observation that AMPK$^{\Delta}$ obtained from a 5 min incubation with the LKB1 complex, which contained only a

fraction of proteoform that had been phosphorylated at Thr172 (Figure 3), could still completely phosphorylate the SAMS peptide within 10 min (Figure 6) provides strong evidence that phosphorylation at Thr172 plays a dominant role in regulating the activity of AMPK$^{\Delta}$.

The Basal Activity of AMPK$^{\Delta}$

The observation that the AMPK$^{\Delta}$ directly purified from *E. coli* was basally phosphorylated at Ser18 prompted us to hypothesize that AMPK$^{\Delta}$ possesses some degree of basal catalytic activity that is independent of phosphorylation at Thr172. Consistent with this hypothesis, we observed that dephosphorylated AMPK$^{\Delta}$ became re-phosphorylated after incubation with ATP in kinase buffer, demonstrating that AMPK$^{\Delta}$ is capable of phosphorylating itself without activation. Furthermore, AMPK$^{\Delta}$ purified directly from *E.coli* was able to phosphorylate SAMS peptide without activating phosphorylation at Thr172, although the phosphorylation level of SAMS peptide was lower than that of SAMS peptide incubated with AMPK$^{\Delta}$ that was activated by LKB1 (Figure 6). Thus, these results confirmed that AMPK$^{\Delta}$ indeed possesses basal activity, which is in agreement with the findings of previous studies [19, 21, 48, 49]. Woods et al. also observed a low level of phosphorylation in bacterially-expressed AMPK complex without incubation with upstream kinase [48]. Using a radioactive ^{32}P labeling approach, Hawley et al. showed that dephosphorylated AMPKα purified from rat liver was able to incorporate ^{32}P-labeled ATP in the absence of upstream kinase [19]. These findings corroborate our own finding that AMPK is indeed basally active although the functional significance of this basal activity remains unclear. Notably, whether the basal activity of the AMPK complex is sufficient to promote autophosphorylation in endogenous AMPKβ under physiological conditions would be of great interest. Given the therapeutic potential of AMPK in treating metabolic disorders such as type 2 diabetes and obesity, as well as other diseases including cardiovascular disease and cancer, a comprehensive understanding of the regulatory mechanisms of AMPK activation could aid the development of AMPK-targeting therapeutics. Recently, autophosphorylation of Ser108 in AMPKβ was reported to be a prerequisite for activation of the AMPK complex by the small molecule A769662, which circumvents the requirement of phosphorylation of Thr172 in the α subunit and constitutes a distinct mechanism for activation of AMPK [50–53]. If the basal activity of the AMPK complex is sufficient to catalyze autophosphorylation of Ser108 in AMPKβ, an endogenous ligand that resembles A769662 would be able to activate AMPK independent of both AMP and phosphorylation of Thr172 by upstream kinases [53]. Future works investigating if endogenous AMPKβ is phosphorylated at Ser108 and whether endogenous ligands exist that are able to activate AMPK like A769662 would be of paramount significance.

Top-Down MS in Combination with In Vitro Phosphorylation as a Tool for Comprehensive Characterization of Protein Phosphorylation

Top-down MS is a powerful tool for proteomics studies and has significant advantages over currently available methods for the investigation of PTMs [27, 28, 30, 33–35, 47, 54]. One major advantage of top-down over bottom-up MS in identifying phosphorylation sites of proteins lies in its complete sequence coverage [27, 28]. As bottom-up MS analyzes peptides instead of proteins, not all the peptides generated are recovered and detected, resulting in partial sequence coverage, which makes bottom-up MS prone to miss important information about phosphorylation and other PTMs in a protein, thus limiting its power to characterize proteins with PTMs [55]. In contrast, since intact proteins are analyzed in the top-down MS approach, all the information, including sequence variants and PTMs, is retained, thereby eliminating the issue of missing information on important PTMs [31]. Another strength of top-down MS is that it can be used to determine the order of modification, which is not feasible for bottom-up MS because protein digestion abolishes information regarding the interrelationship between PTMs on different parts of a protein [31]. Furthermore, as intact proteins are far larger than modifications, the ionization efficiency is minimally influenced (whereas for small peptides, modifications, such as phosphorylation, can significantly influence ionization and thus compromise its accuracy in assessing relative abundance of protein modifications); this enables top-down MS to provide a comprehensive visualization of all the proteoforms of a gene product and allows quantitative assessment of the stoichiometry of protein phosphorylation and other modifications by top-down MS, which is impossible to achieve using the bottom-up MS approach [30].

The approach combining in vitro phosphorylation assay with top-down MS we described here has unique advantages over the conventional methods to study phosphorylation reaction. In vitro phosphorylation assays using radiolabeled [γ-^{32}P] ATP are commonly used to study the phosphorylation reaction and measure protein kinase activity [3]; however, this approach has several significant drawbacks, including safety concerns over the use of radioactive reagents and the inability to locate the phosphorylation sites on the phosphorylated substrate [56]. In contrast, our approach has the following the advantages: (1) the use of normal ATP instead of radiolabeled [γ-^{32}P] ATP eliminates safety concerns; (2) the use of top-down MS as the detection method not only provides the holistic view of the presence and the abundance of differentially phosphorylated substrates but also allows for precise localization of phosphorylation sites in each of the differentially phosphorylated substrates [34, 47, 54]; (3) as demonstrated in our study (Figure 3), top-down MS analysis of the reaction at different time points allows for tracking of the progress of the reaction (i.e., it allows

for tracking of changes in the abundance of differentially phosphorylated protein species as the reaction proceeds). This also allows the sequential order of phosphorylation events to be determined. In our case, it was evident that AMPK$^{\Delta}$ was phosphorylated at Ser18 upon purification, then it became phosphorylated at Thr196 (equivalent to Thr172 in the endogenous AMPK) when incubated with the LKB1/STRAD/MO25 complex, and followed by phosphorylation of Ser22. Thus our approach represents a powerful alternative to study protein phosphorylation and could have broad application to any other enzyme-substrate system.

Most importantly, owing to the unique capacity of top-down MS to identify phosphorylation sites without a priori knowledge, information gained by studying protein phosphorylation using top-down MS provides novel insights to the study of complex signaling mechanisms. Using top-down MS approach, we previously determined that AMPK was able to phosphorylate cardiac troponin I at Ser150 [40]. Subsequent investigation showed that troponin I is phosphorylated at Ser150 in vivo in response to AMPK activation, and that this phosphorylation leads to an increase in the Ca^{2+} sensitivity of the myofilament as well as enhanced cardiac contractility [57, 58]. Therefore, we envision that top-down MS becomes an indispensable tool in the near future in assisting biologists to unravel the complex mechanisms involved in kinase activation and kinase-mediated signaling pathways.

Conclusion

In this study, we have comprehensively analyzed AMPK$^{\Delta}$ expressed in and purified from *E. coli* and after in vitro phosphorylation using top-down MS. We discovered that AMPK$^{\Delta}$ purified from *E. coli* is phosphorylated at Ser18 in the His-tag region and have shown that this bacterially expressed AMPK$^{\Delta}$ can phosphorylate itself and its substrate without activation, thus demonstrating that AMPK$^{\Delta}$ has basal activity, which is independent of Thr172 phosphorylation. Incubation of AMPK$^{\Delta}$ with LKB1 promoted rapid phosphorylation at Thr196 (equivalent to Thr172 in endogenous AMPK) and dramatically increased the activity of AMPK$^{\Delta}$, suggesting that phosphorylation of Thr172 in the kinase domain is the predominant mechanistic event that regulates the activity of AMPK$^{\Delta}$. Additionally, our study demonstrated that top-down MS is a powerful method for monitoring in vitro phosphorylation reactions and dissecting PTM-associated mechanisms regulating protein activity and function.

Acknowledgment

The authors thank Dr. Wei Guo for his training on the molecular cloning used in this study, and all the members in the Ge lab for helpful discussion. The authors are particularly grateful to Nicole Lane for her help in revision of the manuscript. Financial support was kindly provided by NIH R01HL096971 and R01HL109810 (to Y.G.).

References

1. Kahn, B.B., Alquier, T., Carling, D., Hardie, D.G.: AMP-activated protein kinase: ancient energy gauge provides clues to modern understanding of metabolism. Cell Metab. **1**, 15–25 (2005)
2. Hardie, D.G.: AMP-activated/SNF1 protein kinases: conserved guardians of cellular energy. Nat. Rev. Mol. Cell Biol. **8**, 774–785 (2007)
3. Carling, D., Mayer, F.V., Sanders, M.J., Gamblin, S.J.: AMP-activated protein kinase: nature's energy sensor. Nat. Chem. Biol. **7**, 512–518 (2011)
4. Hardie, D.G., Ross, F.A., Hawley, S.A.: AMPK: a nutrient and energy sensor that maintains energy homeostasis. Nat. Rev. Mol. Cell Biol. **13**, 251–262 (2012)
5. Musi, N., Hirshman, M.F., Arad, M., Xing, Y., Fujii, N., Pomerleau, J., Ahmad, F., Berul, C.I., Seidman, J.G., Tian, R., Goodyear, L.J.: Functional role of AMP-activated protein kinase in the heart during exercise. FEBS Lett. **579**, 2045–2050 (2005)
6. Baron, S.J., Li, J., Russell, R.R., Neumann, D., Miller, E.J., Tuerk, R., Wallimann, T., Hurley, R.L., Witters, L.A., Young, L.H.: Dual mechanisms regulating AMPK kinase action in the ischemic heart. Circ. Res. **96**, 337–345 (2005)
7. Young, L.H., Li, J., Baron, S.J., Russell, R.R.: AMP-activated protein kinase: a key stress signaling pathway in the heart. Trends Cardiovasc. Med. **15**, 110–118 (2005)
8. Shirwany, N.A., Zou, M.-H.: AMPK: a cellular metabolic and redox sensor. A minireview. Front. Biosci. Landmark Ed. **19**, 447–474 (2014)
9. Dolinsky, V.W., Dyck, J.R.B.: Role of AMP-activated protein kinase in healthy and diseased hearts. Am. J. Physiol. Heart Circ. Physiol. **291**, H2557–H2569 (2006)
10. Li, J., Coven, D.L., Miller, E.J., Hu, X., Young, M.E., Carling, D., Sinusas, A.J., Young, L.H.: Activation of AMPK alpha- and gamma-isoform complexes in the intact ischemic rat heart. Am. J. Physiol. Heart Circ. Physiol. **291**, H1927–H1934 (2006)
11. Shirwany, N.A., Zou, M.-H.: AMPK in cardiovascular health and disease. Acta Pharmacol. Sin. **31**, 1075–1084 (2010)
12. Kim, M., Tian, R.: Targeting AMPK for cardiac protection: opportunities and challenges. J. Mol. Cell. Cardiol. **51**, 548–553 (2011)
13. Davies, S.P., Hawley, S.A., Woods, A., Carling, D., Haystead, T.A., Hardie, D.G.: Purification of the AMP-activated protein kinase on ATP-gamma-sepharose and analysis of its subunit structure. Eur. J. Biochem. FEBS **223**, 351–357 (1994)
14. Hardie, D.G., Carling, D., Carlson, M.: The AMP-activated/SNF1 protein kinase subfamily: metabolic sensors of the eukaryotic cell? Annu. Rev. Biochem. **67**, 821–855 (1998)
15. Steinberg, G.R., Kemp, B.E.: AMPK in health and disease. Physiol. Rev. **89**, 1025–1078 (2009)
16. Woods, A., Salt, I., Scott, J., Hardie, D.G., Carling, D.: The alpha1 and alpha2 isoforms of the AMP-activated protein kinase have similar activities in rat liver but exhibit differences in substrate specificity *in vitro*. FEBS Lett. **397**, 347–351 (1996)
17. Crute, B.E., Seefeld, K., Gamble, J., Kemp, B.E., Witters, L.A.: Functional domains of the alpha1 catalytic subunit of the AMP-activated protein kinase. J. Biol. Chem. **273**, 35347–35354 (1998)
18. Pang, T., Xiong, B., Li, J.-Y., Qiu, B.-Y., Jin, G.-Z., Shen, J.-K., Li, J.: Conserved alpha-helix acts as autoinhibitory sequence in AMP-activated protein kinase alpha subunits. J. Biol. Chem. **282**, 495–506 (2007)
19. Hawley, S.A., Davison, M., Woods, A., Davies, S.P., Beri, R.K., Carling, D., Hardie, D.G.: Characterization of the AMP-activated protein kinase kinase from rat liver and identification of threonine 172 as the major site at which it phosphorylates AMP-activated protein kinase. J. Biol. Chem. **271**, 27879–27887 (1996)
20. Zaha, V.G., Young, L.H.: AMP-activated protein kinase regulation and biological actions in the heart. Circ. Res. **111**, 800–814 (2012)
21. Stein, S.C., Woods, A., Jones, N.A., Davison, M.D., Carling, D.: The regulation of AMP-activated protein kinase by phosphorylation. Biochem. J. **345**(Pt 3), 437–443 (2000)
22. Smith, L.M., Kelleher, N.L.: Consortium for Top Down Proteomics: Proteoform: a single term describing protein complexity. Nat. Methods **10**, 186–187 (2013)

23. Kelleher, N.L., Lin, H.Y., Valaskovic, G.A., Aaserud, D.J., Fridriksson, E.K., McLafferty, F.W.: Top down versus bottom up protein characterization by tandem high-resolution mass spectrometry. J. Am. Chem. Soc. **121**, 806–812 (1999)
24. Ge, Y., Lawhorn, B.G., ElNaggar, M., Strauss, E., Park, J.-H., Begley, T.P., McLafferty, F.W.: Top down characterization of larger proteins (45 kDa) by electron capture dissociation mass spectrometry. J. Am. Chem. Soc. **124**, 672–678 (2002)
25. Sze, S.K., Ge, Y., Oh, H., McLafferty, F.W.: Top-down mass spectrometry of a 29-kDa protein for characterization of any posttranslational modification to within one residue. Proc. Natl. Acad. Sci. U. S. A. **99**, 1774–1779 (2002)
26. Han, X., Jin, M., Breuker, K., McLafferty, F.W.: Extending top-down mass spectrometry to proteins with masses greater than 200 kilodaltons. Science **314**, 109–112 (2006)
27. Siuti, N., Kelleher, N.L.: Decoding protein modifications using top-down mass spectrometry. Nat. Methods **4**, 817–821 (2007)
28. Ryan, C.M., Souda, P., Bassilian, S., Ujwal, R., Zhang, J., Abramson, J., Ping, P., Durazo, A., Bowie, J.U., Hasan, S.S., Baniulis, D., Cramer, W.A., Faull, K.F., Whitelegge, J.P.: Post-translational modifications of integral membrane proteins resolved by top-down Fourier transform mass spectrometry with collisionally activated dissociation. Mol. Cell. Proteom. **9**, 791–803 (2010)
29. Tran, J.C., Zamdborg, L., Ahlf, D.R., Lee, J.E., Catherman, A.D., Durbin, K.R., Tipton, J.D., Vellaichamy, A., Kellie, J.F., Li, M., Wu, C., Sweet, S.M.M., Early, B.P., Siuti, N., LeDuc, R.D., Compton, P.D., Thomas, P.M., Kelleher, N.L.: Mapping intact protein isoforms in discovery mode using top-down proteomics. Nature **480**, 254–258 (2011)
30. Zhang, H., Ge, Y.: Comprehensive analysis of protein modifications by top-down mass spectrometry. Circ. Cardiovasc. Genet. **4**, 711 (2011)
31. Gregorich, Z.R., Ge, Y.: Top-down proteomics in health and disease: challenges and opportunities. Proteomics **14**, 1195–1210 (2014)
32. Peng, Y., Ayaz-Guner, S., Yu, D., Ge, Y.: Top-down mass spectrometry of cardiac myofilament proteins in health and disease. Proteom. Clin. Appl. **8**, 554–568 (2014)
33. Zabrouskov, V., Ge, Y., Schwartz, J., Walker, J.W.: Unraveling molecular complexity of phosphorylated human cardiac troponin I by top down electron capture dissociation/electron transfer dissociation mass spectrometry. Mol. Cell. Proteom. **7**, 1838–1849 (2008)
34. Ge, Y., Rybakova, I.N., Xu, Q., Moss, R.L.: Top-down high-resolution mass spectrometry of cardiac myosin binding protein C revealed that truncation alters protein phosphorylation state. Proc. Natl. Acad. Sci. U. S. A. **106**, 12658–12663 (2009)
35. Zhang, J., Guy, M.J., Norman, H.S., Chen, Y.-C., Xu, Q., Dong, X., Guner, H., Wang, S., Kohmoto, T., Young, K.H., Moss, R.L., Ge, Y.: Top-down quantitative proteomics identified phosphorylation of cardiac troponin I as a candidate biomarker for chronic heart failure. J. Proteome Res. **10**, 4054–4065 (2011)
36. Dong, X., Sumandea, C.A., Chen, Y.-C., Garcia-Cazarin, M.L., Zhang, J., Balke, C.W., Sumandea, M.P., Ge, Y.: Augmented phosphorylation of cardiac troponin I in hypertensive heart failure. J. Biol. Chem. **287**, 848–857 (2012)
37. Peng, Y., Chen, X., Zhang, H., Xu, Q., Hacker, T.A., Ge, Y.: Top-down targeted proteomics for deep sequencing of tropomyosin isoforms. J. Proteome Res. **12**, 187–198 (2013)
38. Peng, Y., Gregorich, Z.R., Valeja, S.G., Zhang, H., Cai, W., Chen, Y.-C., Guner, H., Chen, A.J., Schwahn, D.J., Hacker, T.A., Liu, X., Ge, Y.: Top-down proteomics reveals concerted reductions in myofilament and Z-disc protein phosphorylation after acute myocardial infarction. Mol. Cell. Proteom. **13**, 2752–2764 (2014)
39. Landgraf, R.R., Goswami, D., Rajamohan, F., Harris, M.S., Calabrese, M.F., Hoth, L.R., Magyar, R., Pascal, B.D., Chalmers, M.J., Busby, S.A., Kurumbail, R.G., Griffin, P.R.: Activation of AMP-activated protein kinase revealed by hydrogen/deuterium exchange mass spectrometry. Struct. Lond. Engl. **21**, 1942–1953 (2013)
40. Sancho Solis, R., Ge, Y., Walker, J.W.: A preferred AMPK phosphorylation site adjacent to the inhibitory loop of cardiac and skeletal troponin I. Protein Sci. **20**, 894–907 (2011)
41. Peng, Y., Yu, D., Gregorich, Z., Chen, X., Beyer, A.M., Gutterman, D.D., Ge, Y.: In-depth proteomic analysis of human tropomyosin by top-down mass spectrometry. J. Muscle Res. Cell Motil. **34**, 199–210 (2013)
42. Guner, H., Close, P.L., Cai, W., Zhang, H., Peng, Y., Gregorich, Z.R., Ge, Y.: MASH Suite: a user-friendly and versatile software interface for high-resolution mass spectrometry data interpretation and visualization. J. Am. Soc. Mass Spectrom. **25**, 464–470 (2014)
43. Gwinn, D.M., Shackelford, D.B., Egan, D.F., Mihaylova, M.M., Mery, A., Vasquez, D.S., Turk, B.E., Shaw, R.J.: AMPK phosphorylation of raptor mediates a metabolic checkpoint. Mol. Cell **30**, 214–226 (2008)
44. Woods, A., Johnstone, S.R., Dickerson, K., Leiper, F.C., Fryer, L.G.D., Neumann, D., Schlattner, U., Wallimann, T., Carlson, M., Carling, D.: LKB1 is the upstream kinase in the AMP-activated protein kinase cascade. Curr. Biol. **13**, 2004–2008 (2003)
45. Hawley, S.A., Boudeau, J., Reid, J.L., Mustard, K.J., Udd, L., Mäkelä, T.P., Alessi, D.R., Hardie, D.G.: Complexes between the LKB1 tumor suppressor, STRAD alpha/beta and MO25 alpha/beta are upstream kinases in the AMP-activated protein kinase cascade. J. Biol. **2**, 28 (2003)
46. Shaw, R.J., Kosmatka, M., Bardeesy, N., Hurley, R.L., Witters, L.A., DePinho, R.A., Cantley, L.C.: The tumor suppressor LKB1 kinase directly activates AMP-activated kinase and regulates apoptosis in response to energy stress. Proc. Natl. Acad. Sci. U. S. A. **101**, 3329–3335 (2004)
47. Ayaz-Guner, S., Zhang, J., Li, L., Walker, J.W., Ge, Y.: In vivo phosphorylation site mapping in mouse cardiac troponin I by high resolution top-down electron capture dissociation mass spectrometry: Ser22/23 are the only sites basally phosphorylated. Biochemistry (Mosc) **48**, 8161–8170 (2009)
48. Woods, A., Vertommen, D., Neumann, D., Turk, R., Bayliss, J., Schlattner, U., Wallimann, T., Carling, D., Rider, M.H.: Identification of phosphorylation sites in AMP-activated protein kinase (AMPK) for upstream AMPK kinases and study of their roles by site-directed mutagenesis. J. Biol. Chem. **278**, 28434–28442 (2003)
49. Mitchelhill, K.I., Michell, B.J., House, C.M., Stapleton, D., Dyck, J., Gamble, J., Ullrich, C., Witters, L.A., Kemp, B.E.: Post-translational modifications of the 5′-AMP-activated protein kinase beta1 subunit. J. Biol. Chem. **272**, 24475–24479 (1997)
50. Sanders, M.J., Ali, Z.S., Hegarty, B.D., Heath, R., Snowden, M.A., Carling, D.: Defining the mechanism of activation of AMP-activated protein kinase by the small molecule A-769662, a member of the thienopyridone family. J. Biol. Chem. **282**, 32539–32548 (2007)
51. Scott, J.W., van Denderen, B.J.W., Jorgensen, S.B., Honeyman, J.E., Steinberg, G.R., Oakhill, J.S., Iseli, T.J., Koay, A., Gooley, P.R., Stapleton, D., Kemp, B.E.: Thienopyridone drugs are selective activators of AMP-activated protein kinase beta1-containing complexes. Chem. Biol. **15**, 1220–1230 (2008)
52. Scott, J.W., Ling, N., Issa, S.M.A., Dite, T.A., O'Brien, M.T., Chen, Z.-P., Galic, S., Langendorf, C.G., Steinberg, G.R., Kemp, B.E., Oakhill, J.S.: Small molecule drug A-769662 and AMP synergistically activate naive AMPK independent of upstream kinase signaling. Chem. Biol. **21**, 619–627 (2014)
53. Viollet, B., Foretz, M., Schlattner, U.: Bypassing AMPK phosphorylation. Chem. Biol. **21**, 567–569 (2014)
54. Zhang, J., Dong, X., Hacker, T.A., Ge, Y.: Deciphering modifications in swine cardiac troponin I by top-down high-resolution tandem mass spectrometry. J. Am. Soc. Mass Spectrom. **21**, 940–948 (2010)
55. Chait, B.T.: Mass spectrometry: bottom-up or top-down? Science **314**, 65–66 (2006)
56. Hastie, C.J., McLauchlan, H.J., Cohen, P.: Assay of protein kinases using radiolabeled ATP: a protocol. Nat. Protoc. **1**, 968–971 (2006)
57. Oliveira, S.M., Zhang, Y.-H., Solis, R.S., Isackson, H., Bellahcene, M., Yavari, A., Pinter, K., Davies, J.K., Ge, Y., Ashrafian, H., Walker, J.W., Carling, D., Watkins, H., Casadei, B., Redwood, C.: AMP-activated protein kinase phosphorylates cardiac troponin I and alters contractility of murine ventricular myocytes. Circ. Res. **110**, 1192–1201 (2012)
58. Chen, S., Zhu, P., Guo, H.-M., Solis, R.S., Wang, Y., Ma, Y., Wang, J., Gao, J., Chen, J.-M., Ge, Y., Zhuang, J., Li, J.: Alpha1 catalytic subunit of AMPK modulates contractile function of cardiomyocytes through phosphorylation of troponin I. Life Sci. **98**, 75–82 (2014)